Using Central Manifold Theorem in the Analysis of Master-Slave Synchronization Networks

José Roberto Castilho Piqueira, Carlos Nehemy Marmo, and Luiz Henrique Alves Monteiro

Abstract: **This work presents a stability analysis of the synchronous state for one-way master-slave time distribution networks with single star topology.**

Using bifurcation theory, the dynamical behavior of second-order phase-locked loops employed to extract the synchronous state in each node is analyzed in function of the constitutive parameters.

Two usual inputs, the step and the ramp phase perturbations, are supposed to appear in the master node and, in each case, the existence and the stability of the synchronous state are studied.

For parameter combinations resulting in non-hyperbolic synchronous states the linear approximation does not provide any information, even about the local behavior of the system. In this case, the center manifold theorem permits the construction of an equivalent vector field representing the asymptotic behavior of the original system in a local neighborhood of these points. Thus, the local stability can be determined.

Index Terms: **Bifurcation, master-slave, network, phase-locked loops, single-star, synchronization, synchronous state.**

I. INTRODUCTION

The main purpose of a time distributing system is to synchronize the phase and the frequency of several oscillators spread over a geographical area [1].

If the synchronization is obtained without the transmission of control signals, the network is called plesiochronous. In this case, each node of the network needs an accurate oscillator, individually aligned. The main advantage of this strategy is the robustness to failures in the node clock circuits.

In order to obtain the same effect with cheaper networks we can use the line signals to carry the clock basis and, in each node, the phase and the frequency of a control signal are reconstructed. This type of network is called synchronous.

If all the nodes give some contribution to the synchronization frequency, the network is called mutually synchronized. If there is any kind of priority on determining the synchronous state, the network is called master-slave.

In a master-slave network, if the master oscillator control signal does not depend on the signals from other nodes, the network is called one-way master-slave (OWMS). If the signal from the master depends on the slave signals, the network is called two-way master-slave (TWMS) [1].

Manuscript received June 30, 2003; approved for publication by Yong Hoon Lee, Division I Division Editor, July 27, 2004.

The authors are with the Departamento de Engenharia de Telecomunicações e Controle, Escola Politécnica, Universidade de São Paulo and with Pós Graduação em Engenharia Elétrica, Universidade Presbiteriana Mackenzie, email: piqueira@lac.usp.br, cnmarmo@ig.com.br, luizm@usp.br.

This work is supported by CNPq.

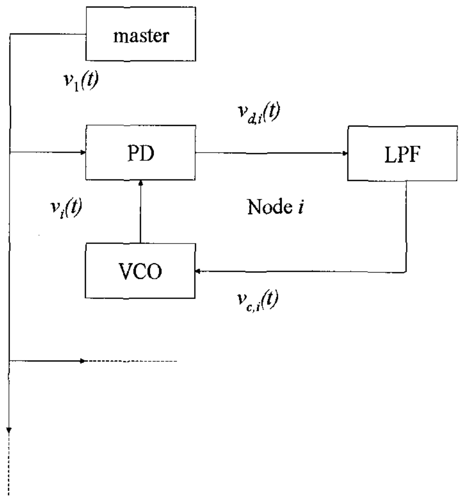

Fig. 1. OWMS single star.

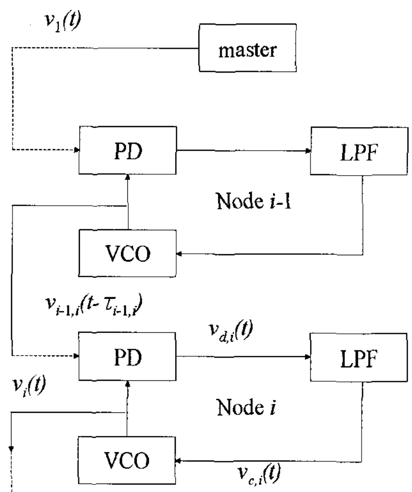

Fig. 2. OWMS single chain.

Our work is about OWMS topologies, i.e., with the control signal transmitted in a single direction. The main oscillator, called master, has its own time and frequency scales, not dependent of the others, called slaves.

When the transmission of the control signal occurs directly from the master to all slaves, the network is called single star (Fig. 1).

When a slave can be controlled by the master or another slave, the topology is called single chain (Fig. 2).

Both of them, OWMS single star and single chain, are easy to implement, with low cost and acceptable reliability. So, they appear in public telecommunication networks, in parallel and

1229-2370/04/$10.00 © 2004 KICS

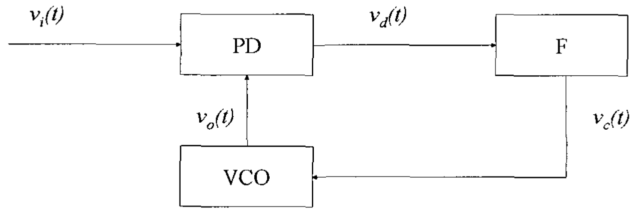

Fig. 3. The phase-locked loop.

distributed computation [2], in robotics [3], and many other engineering applications [1], [4].

The maximum number of slaves can be calculated for a single chain, in order to obtain a good performance of the clock extraction system, using analytical tools [5] but we are not considering this problem here.

Here we consider the OWMS single star with the master as a high quality atomic oscillator, and the slaves are composed by second order phase-locked loops (PLLs).

PLLs are electronic circuits designed to extract the time signal from line signals. They were developed in 1932 by H. de Bellescize and the first commercial application was on television sets, in 1943 [6]. Nowadays, they are extensively used for constructing clock synthesizers for computer and in communication applications [7].

In our study, we choose second-order PLLs because they can present satisfactory transient response to step and ramp phase inputs, and avoid periodic and chaotic attractors for the phase and frequency errors.

If it is necessary to improve the transient response of the networks, it is usual to increase the PLL's order. However, due to the nonlinearity, self-sustained error oscillations [8]–[10] can appear and, depending on the order; Arnold diffusion also appears [11]. These phenomena limit the lock-in range of the nodes along the network.

A PLL is composed by three elements, connected in a closed loop: A phase detector (PD), a low-pass filter (LPF), and a voltage controlled oscillator (VCO), as shown in Fig. 3.

The idea is to synchronize the signal generated by the VCO and the external signal, making their phase difference a constant value, or equivalently, their frequency difference equal to zero. In this situation, we say that the node is in a synchronous state.

The existence and the stability of the synchronous state depend on node and line parameters, and on the function that represents the changes of the master phase signal. Two types of phase changing functions are considered here, step and ramp, because they are usual in real applications.

We start presenting the differential equations representing the slave node PLL dynamics for the OWMS single star networks. The equations are of second-order, nonlinear, and autonomous.

The vector fields corresponding to these equations are studied and the linear approximation around the equilibrium points captures the main aspects related to synchronous state stability. But, for some practical combinations of parameters, a synchronous state corresponding to an eigenvalue with zero real part (non hyperbolic point) can be obtained and, consequently, the linear approximation is not sufficient to provide useful conclusions about the synchronous state.

Then, we use the center manifold theorem, constructing an equivalent vector field that reveals the asymptotic behavior of the original system in the neighborhood of non-hyperbolic equilibrium points [12], [13].

Bifurcation diagrams associate parameter space regions to dynamical behaviors of OWMS single-star networks. Such diagrams are presented here.

II. SECOND-ORDER PLL IN OWMS-SINGLE STAR

In the single star architecture, the slaves are directly connected to the master and, then, the equations are of the same type for all nodes.

The input and output signals in all nodes are considered to have a periodic free-running term with central angular frequency ω_0.

The master signal $v_1(t)$, with amplitude V_1 and phase Φ_1 is transmitted from the master to the ith slave with a τ_{1i} delay, being the input of the PD for all slave PLLs and given by:

$$\begin{aligned} v_1(t-\tau_{1i}) &= V_1\sin[\Phi_1(t-\tau_{1i})] \\ &= V_1\sin[\omega_0(t-\tau_{1i})+\theta_1(t-\tau_{1i})]. \end{aligned} \quad (1)$$

The VCO signal $v_i(t)$ of the ith slave, with amplitude V_i and phase Φ_i is given by

$$\begin{aligned} v_i(t) &= V_i\cos[\Phi_i(t)] \\ &= V_i\cos[\omega_0(t)+\theta_i(t)], \end{aligned} \quad (2)$$

with θ_1 expressing how the phase of the master depends on time and θ_i, the ith slave adjustable phase.

Neglecting the double-frequency terms [7], the PD output, considered a signal multiplier, is expressed by:

$$v_{d,i}(t) = \frac{K_{m,i}V_1V_i}{2}\sin[\theta_1(t-\tau_{1i})-\theta_i(t)-\omega_0\tau_{1i}], \quad (3)$$

where $K_{m,i}$ is the PD gain.

The filter is considered to be a linear first-order lag [14] with transfer function:

$$F(s) = \frac{1}{RCs+1}, \quad (4)$$

where the product RC means the filter time constant.

In order to have better transient responses higher order filters can be considered. Here they are not being analyzed because additional bifurcations appear, as shown in [15].

The phase of the VCO signal is controlled by the filter output $v_c(t)$ according to:

$$\dot{\theta}_i = K_i v_c(t), \quad (5)$$

where K_i is the VCO gain.

Using (3) and (5) in the transfer function of the filter (4), we have the dynamics of the phase of the VCO described by the following ordinary nonlinear equation:

$$\ddot{\theta}_i + \mu_{1,i}\,\dot{\theta}_i = \mu_{1,i}\mu_{2,i}\sin\left(\theta_1(t-\tau_{1i})-\theta_i(t)-\omega_0\tau_{1i}\right), \quad (6)$$

where $\mu_{1,i} = \frac{1}{RC}$ and $\mu_{2,i} = \frac{K_i K_{m,i} V_1 V_i}{2}$.

In order to formulate the problem, we have to define two types of phase errors: The first, φ_{ii}, between the input and the VCO signal of the ith node and the second, φ_{1i}, between the VCO signal of the ith node and the master.

That is

$$\varphi_{ii}(t) = \theta_1(t-\tau_{1i}) - \theta_i(t) - \omega_0\tau_{1i}, \quad (7)$$
$$\varphi_{1i}(t) = \theta_1(t) - \theta_i(t). \quad (8)$$

If one replaces phase errors (7) and (8) and their derivatives in (6), the dynamics is described by

$$\begin{cases} \ddot{\varphi}_{ii}(t) + \mu_{1,i}\,\dot{\varphi}_{ii}(t) + \mu_{1,i}\mu_{2,i}\sin[\varphi_{ii}(t)] \\ \qquad = \ddot{\theta}_1(t-\tau_{1i}) + \mu_{1,i}\,\dot{\theta}_1(t-\tau_{1i}), \\ \ddot{\varphi}_{1i}(t) + \mu_{1,i}\,\dot{\varphi}_{1i}(t) + \mu_{1,i}\mu_{2,i}\sin[\varphi_{ii}(t)] \\ \qquad = \ddot{\theta}_1(t) + \mu_{1,i}\,\dot{\theta}_1(t). \end{cases} \quad (9)$$

A. Synchronous State Stability with Step Input

If the input phase is a step, we can write for each node i, and considering $t > \tau_{1i}$:

$$\begin{cases} \ddot{\varphi}_{ii}(t) + \mu_{1,i}\,\dot{\varphi}_{ii}(t) + \mu_{1,i}\mu_{2,i}\sin[\varphi_{ii}(t)] = 0 \\ \ddot{\varphi}_{1i}(t) + \mu_{1,i}\,\dot{\varphi}_{1i}(t) + \mu_{1,i}\mu_{2,i}\sin[\varphi_{ii}(t)] = 0. \end{cases} \quad (10)$$

In order to normalize the equations, we change the independent variable t by $T \equiv \mu_{1,i}t$. Using primes to indicate the derivatives related to T, (10) becomes

$$\begin{cases} \varphi_{ii}''(T) + \varphi_{ii}'(T) + \mu_i\sin[\varphi_{ii}(T)] = 0 \\ \varphi_{1i}''(T) + \varphi_{1i}'(T) + \mu_i\sin[\varphi_{ii}(T)] = 0, \end{cases} \quad (11)$$

where $\mu_i = \dfrac{\mu_{2,i}}{\mu_{1,i}}$.

Choosing convenient state variables, a three dimensional system equation describes the dynamics of the each slave node as

$$\begin{cases} x_1 = \varphi_{1i}' \\ x_2 = \varphi_{ii} \\ x_3 = \varphi_{ii}' \end{cases} \Longrightarrow \begin{cases} x_1' = -x_1 - \mu_i\sin x_2 \\ x_2' = x_3 \\ x_3' = -x_3 - \mu_i\sin x_2. \end{cases} \quad (12)$$

Equation (12) has two equilibrium points: $P_1 = (0,0,0)$ and $P_2 = (0,-\pi,0)$.

Calculating the eigenvalues associated to the linear approximation in P_1, we obtain $\lambda_1 = -1$ and $\lambda_{2,3} = \dfrac{-1 \pm \sqrt{1-4\mu_i}}{2}$.

As usual, we define stable sub-space E^s as the space spanned by the eigenvectors corresponding to the eigenvalues with negative real parts, unstable sub-space E^u as the space spanned by the eigenvectors corresponding to the eigenvalues with positive real parts and central sub-space (E^c) as the space spanned by the eigenvectors corresponding to the eigenvalues with zero real parts [12], [13].

As whole state space is generated by the union of E^s, E^u, and E^c, by observing all possible values that the parameter μ_i can assume, the stability of P_1 is given by

- For $\mu_i > 0 \Rightarrow dim(E^s) = 3 \Rightarrow P_1$ is asymptotically stable.
- For $\mu_i < 0 \Rightarrow dim(E^s) = 2$, $dim(E^u) = 1 \Rightarrow P_1$ is unstable.
- For $\mu_i = 0 \Rightarrow dim(E^s) = 2$, $dim(E^c) = 1 \Rightarrow$ nothing can be concluded from the linear approximation.

The changing in the qualitative behavior of the system (bifurcation) in $\mu_i = 0$ implies that the application of center manifold theorem is possible to study the dynamics restricted to E^c [12], [13].

So, we include in (12) μ_i as a new dependent variable.

Using the Jordan form and the Taylor expansion $\sin x_2 \approx x_2$ around $x_2 = 0$, with the set of eigenvectors as the base of the state space, we have

$$\begin{bmatrix} v_1' \\ v_2' \\ v_3' \end{bmatrix} = \begin{bmatrix} -1 & 0 & 0 \\ 0 & -1 & 0 \\ 0 & 0 & 0 \end{bmatrix} \begin{bmatrix} v_1 \\ v_2 \\ v_3 \end{bmatrix} + \begin{bmatrix} -\mu_i(-v_1+v_3) \\ -\mu_i(-v_1+v_3) \\ -\mu_i(-v_1+v_3) \end{bmatrix},$$

and

$$\mu_i' = 0. \quad (13)$$

The center manifold related to (13) can be represented by

$$W_{loc}^c(0) = \{ (v_1, v_2, v_3, \mu_i) \in \Re^4 / v_1 = h_1(x,\mu_i), \; v_2 = h_2(x,\mu_i), \; v_3 = x, \; h_j(0,0) = 0, \; Dh_j(0,0), \; j = 1,2\}, \quad (14)$$

for x and μ_i sufficiently small, with $h(x,\mu) : E^c \times R \longrightarrow E^s$ being a function expressing analytically the center manifold. The conditions $h_j(0,0) = 0$, $Dh_j(0,0)$, $j = 1,2$ imply that the center manifold is tangent to E^c at the equilibrium point.

Additionally, in order to satisfy the original differential equation, (14) needs to be according to

$$D_x h(x,\mu_i)[Ax + f(x, h(x,\mu_i), \mu_i)] - Bh(x,\mu_i) - g(x, h(x,\mu_i), \mu_i) = 0, \quad (15)$$

where A is a $c \times c$ matrix having eigenvalues with zero real part, B is a $s \times s$ matrix having eigenvalues with negative real part, and f and g are the nonlinear terms to be studied.

The dynamics described by (13) does not depend on $v_2 = h_2(x,\mu_i)$, therefore, we need only to estimate $v_1 = h_1(x,\mu_i)$, using a polynomial approximation, according to Henry-Carr theorem [12], [16], as following

$$h_1(x,\mu_i) = ax^2 + bx\mu_i + c\mu_i^2. \quad (16)$$

Substituting (16) into (17) and using (13), then

$$h_1(x,\mu_i) = -\mu_i x. \quad (17)$$

Replacing (17) into (13), the vector field, restricted to the center manifold, can be represented by

$$\begin{cases} x' = -\mu_i x \\ \mu_i' = 0. \end{cases} \quad (18)$$

The construction of the bifurcation diagram corresponding to (18) is shown in Fig. 4, indicating convergence to the equilibrium point for $\mu_i > 0$ and divergence for $\mu_i < 0$. As the parameter μ_i is the PLL gain normalized to the cut-off frequency of

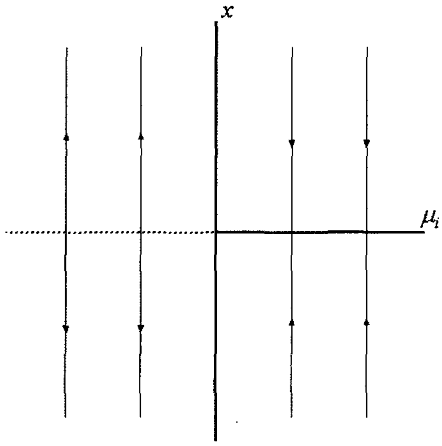

Fig. 4. Single star with step input: Bifurcation diagram.

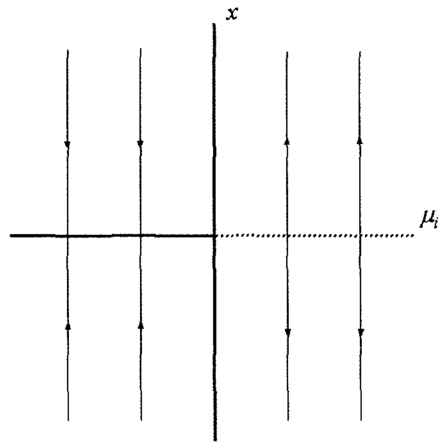

Fig. 5. Single star with step input: Bifurcation diagram.

the filter and is always positive, if it is conveniently chosen not so close to zero, the point P_1 is asymptotically stable.

Following the same procedure, we can study the behavior of the system around P_2.

The eigenvalues associated to the linear approximation in P_2 are $\lambda_1 = -1$ and $\lambda_{2,3} = \frac{-1 \pm \sqrt{1+4\mu_i}}{2}$.

Observing all possible values that the parameter μ_i can assume, the stability of P_2 is given by

- For $\mu_i < 0 \Rightarrow dim(E^s) = 3 \Rightarrow P_1$ is asymptotically stable.
- For $\mu_i > 0 \Rightarrow dim(E^s) = 2$, $dim(E^u) = 1 \Rightarrow P_1$ is unstable.
- For $\mu_i = 0 \Rightarrow dim(E^s) = 2$, $dim(E^c) = 1 \Rightarrow$ nothing can be concluded from the linear approximation.

Once more, the bifurcation in $\mu_i = 0$ implies that the application of the center manifold theorem can be necessary to study the dynamics restricted to E^c.

Including μ_i as a new dependent variable and using Taylor expansion around $x_2 = -\pi$, we have, using the Jordan form translated to the origin

$$\begin{bmatrix} v_1' \\ v_2' \\ v_3' \end{bmatrix} = \begin{bmatrix} -1 & 0 & 0 \\ 0 & -1 & 0 \\ 0 & 0 & 0 \end{bmatrix} \begin{bmatrix} v_1 \\ v_2 \\ v_3 \end{bmatrix} + \begin{bmatrix} +\mu_i(-v_1+v_3) \\ +\mu_i(-v_1+v_3) \\ +\mu_i(-v_1+v_3) \end{bmatrix},$$

and

$$\mu_i' = 0. \tag{19}$$

Therefore, repeating steps (14), (15), and (16), we obtain

$$h_1(x, \mu_i) = +\mu_i x. \tag{20}$$

Replacing (20) into (19), the vector field, restricted to the center manifold, is given by

$$\begin{cases} x' = +\mu_i x \\ \mu_i' = 0. \end{cases} \tag{21}$$

The construction of the bifurcation diagram corresponding to (21) is shown in Fig. 5, indicating convergence to the equilibrium point for $\mu_i < 0$ and divergence for $\mu_i > 0$. As the parameter μ_i is the PLL gain normalized to the cut-off frequency of the filter and is always positive, if it is conveniently chosen not so close to zero, the point P_2 is unstable.

Therefore, we conclude that the OWMS single-star network presents an asymptotically stable synchronous state with zero phase and frequency errors for positive and not too small values of μ_i, when the phase input is a step signal.

B. Synchronous State Stability with Ramp Input

Using a ramp input, we can write for $t > \tau_{1i}$:

$$\begin{cases} \ddot{\varphi}_{ii}(t) + \mu_{1,i}\dot{\varphi}_{ii}(t) + \mu_{1,i}\mu_{2,i}\sin[\varphi_{ii}(t)] = \mu_{1,i}\Omega \\ \ddot{\varphi}_{1i}(t) + \mu_{1,i}\dot{\varphi}_{1i}(t) + \mu_{1,i}\mu_{2,i}\sin[\varphi_{ii}(t)] = \mu_{1,i}\Omega, \end{cases} \tag{22}$$

where Ω is the angular coefficient of the ramp.

Repeating the procedure used for the step input, we change the independent variable t by $T = \mu_{1,i}t$ and use primes to indicate the derivatives related to T. Therefore, system (22) becomes

$$\begin{cases} \varphi_{ii}''(T) + \varphi_{ii}'(T) + \mu_i \sin[\varphi_{ii}(T)] = \bar{\Omega} \\ \varphi_{1i}''(T) + \varphi_{1i}'(T) + \mu_i \sin[r\varphi_{ii}(T)] = \bar{\Omega}, \end{cases} \tag{23}$$

where $\mu_i = \frac{\mu_{2,i}}{\mu_{1,i}}$ and $\bar{\Omega} = \frac{\Omega}{\mu_i}$.

Choosing the convenient state variables, a third order equation describes the PLL dynamics, as following

$$\begin{cases} x_1 = \varphi_{1i}' \\ x_2 = \varphi_{ii} \\ x_3 = \varphi_{ii}' \end{cases} \Longrightarrow \begin{cases} x_1' = \bar{\Omega} - x_1 - \mu_i \sin x_2 \\ x_2' = x_3 \\ x_3' = \bar{\Omega} - x_3 - \mu_i \sin x_2 . \end{cases} \tag{24}$$

Therefore, we have three possibilities

- $\bar{\Omega} > \mu_i \Rightarrow$ there is no equilibrium point.
- $\bar{\Omega} < \mu_i \Rightarrow$ there are two equilibrium points $P_{1,2} = \left(0, \pm \arccos\sqrt{1 - \left(\frac{\bar{\Omega}}{\mu_i}\right)^2}, 0\right)$.

The eigenvalues associated to the linear approximation in P_1 are

$$\lambda_1 = -1 \text{ and } \lambda_{2,3} = \frac{-1 \pm \sqrt{1 - 4\sqrt{\mu_i^2 - \bar{\Omega}^2}}}{2}.$$

Therefore, P_1 is asymptotically stable, because $\lambda_1 \in \Re_-$ and $\lambda_{2,3} \in \Re_-$ or $\lambda_2 = \lambda_3^*$ with $\Re(\lambda_{2,3}) < 0$.
The eigenvalues associated to the linear approximation in P_2 are

$$\lambda_1 = -1 \text{ and } \lambda_{2,3} = \frac{-1 \pm \sqrt{1 + 4\sqrt{\mu_i^2 - \bar{\Omega}^2}}}{2}.$$

Therefore, P_2 is unstable, because $\lambda_1 \in \Re_-$ and $\lambda_{2,3} \in \Re_+$.

- $\bar{\Omega} = \mu_i \Rightarrow$ there is one equilibrium point: $P = \left(0, \frac{\pi}{2}, 0\right)$.

The eigenvalues associated to the linear approximation in P are

$$\lambda_{1,2} = -1 \text{ and } \lambda_3 = 0$$

Therefore, P is a non hyperbolic equilibrium point. Once more, the bifurcation detected in $\mu_i = 0$ implies the application of the center manifold theorem, in order to study the dynamics.

Using the Taylor expansion of the sine function $\sin x_2 \approx 1 + \frac{1}{2}(x_2 - \frac{\pi}{2})$ around $x_2 = \frac{\pi}{2}$, we can rewrite the system (24) in the canonical Jordan form, translated to the origin

$$\begin{bmatrix} v_1' \\ v_2' \\ v_3' \end{bmatrix} = \begin{bmatrix} -1 & 0 & 0 \\ 0 & -1 & 0 \\ 0 & 0 & 0 \end{bmatrix} \begin{bmatrix} v_1 \\ v_2 \\ v_3 \end{bmatrix} + \begin{bmatrix} \frac{\mu_i}{2}(-v_1 + v_3)^2 \\ \frac{\mu_i}{2}(-v_1 + v_3)^2 \\ \frac{\mu_i}{2}(-v_1 + v_3)^2 \end{bmatrix}. \quad (25)$$

Thus, there exists a center manifold for (25) that can, locally, be represented as follows

$$W_{loc}^c(0) = \{ (v_1, v_2, v_3,) \in \Re^3 | v_1 = h_1(x), \\ v_2 = h_2(x), v_3 = x, h_j(0) = 0, Dh_j(0), j = 1, 2 \}, \quad (26)$$

for x sufficiently small.

The center manifold given by (26) must satisfy

$$D_x h(x)[Ax + f(x, h(x)] \\ -Bh(x) - g(x, h(x)) = 0, \quad (27)$$

where A is a $c \times c$ matrix having eigenvalues with zero real part, B is a $s \times s$ matrix having eigenvalues with negative real part, and f and g are the corresponding nonlinear terms.

Now, we want to compute the center manifold and derive the vector field on it. Since the dynamics described by (25) does not depend on $v_2 = h_2(x, \mu_i)$, we need only estimate $v_1 = h_1(x, \mu_i)$.

We try a third-order polynomial

$$h_1(x) = ax^3 + bx^2. \quad (28)$$

Substituting (28) into (27) and using (25), then

$$h_1(x) = -\mu_i^2 x^3 + \frac{\mu_i}{2} x^2. \quad (29)$$

Finally, substituting (29) into (25), the vector field restricted to the center manifold, neglecting terms higher than $\vartheta(x^4)$, is given by

$$x' = -\frac{\mu_i^2}{2} x^3 + \frac{\mu_i}{2} x^2. \quad (30)$$

The construction of the bifurcation diagram corresponding to (30) is shown in Fig. 6, indicating convergence to the equilibrium point for $\mu_i > 0$ and divergence for $\mu_i < 0$. As the parameter μ_i is the PLL gain normalized to the cut-off frequency of the filter and is always positive, if it is conveniently chosen not so close to zero, there is an asymptotically stable equilibrium point for the network.

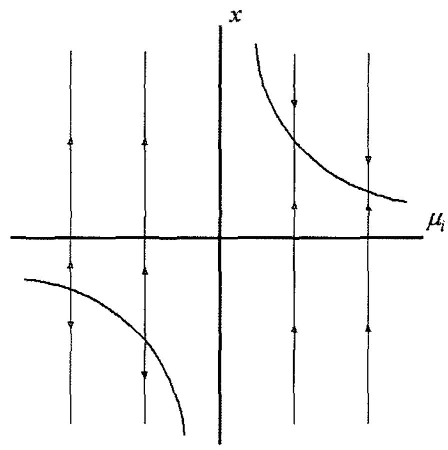

Fig. 6. Single star with ramp input: Bifurcation diagram.

It is interesting to notice that phase ramp inputs can be tracked in OWMS single star networks if the PLL gain of each node (μ_i) is greater than the ramp inclination (Ω). The synchronous state has non zero phase error and zero frequency error.

III. CONCLUSIONS

Using the center manifold theorem is a useful tool in order to establish synchronous state stability conditions for single star OWMS networks in a non-hyperbolic equilibrium point.

Several relations among electrical parameters and possible behaviors of the time regeneration system were obtained here, allowing us to choose parameters for network designing.

The OWMS single star architecture presents, for sufficiently large gains of the PLLs, zero phase and zero frequency error asymptotically stable synchronous state, if the phase input is a step.

Furthermore, considering ramp inputs, for sufficiently large gains of the PLLs, a non zero phase error and zero frequency error asymptotically stable synchronous state appears, if the gain of the PLL nodes is greater than the ramp inclination.

REFERENCES

[1] W. C. Lindsey *et al.*, "Network syncronization," *Proc. IEEE* , vol. 73, no 10, pp. 1445–1467, 1972.
[2] G. Shao, F. Berman, and R. Wolski, "Master/slave computing on the grid," in *Proc. IEEE 21st COMPSAC*, 2000.
[3] W. C. Lee *et al.*, "The distributed controller architecture for a masterarm and its application to teleoperation with force feedback," in *Proc. IEEE International Conference on Robotics & Automation*, Detroit, Michigan-EUA, 1999, pp. 213–218.
[4] S. Sohail and G. Raj, "Replication of multimedia data using master-slave architecture," in *Proc. IEEE 21st COMPSAC*, 1997.
[5] L. H. A. Monteiro, R. V. dos Santos, and J. R. C. Piqueira, "Estimating the critical number of slave nodes in a single-chain PLL network," *IEEE Comun. Lett.*, vol. 7, no. 9, pp. 449–450, 2003.
[6] L. H. A Monteiro, *Sistemas Dinâmicos*, São Paulo-Brazil, Editora Livraria da Física, 2002.
[7] J. R. C. Piqueira and L. H. A. Monteiro, "Considering second-harmonic terms in the operation of the phase detector for second order phase-locked loop," *IEEE Trans. Circuits Syst. I*, vol. 50, no. 6, pp. 805–809, 2003.

[8] T. Endo and L. A. Chua, "Chaos from phase-locked loops," *IEEE Trans. Circuits Syst.*, vol. 35, pp. 987–1003, 1988.
[9] T. Endo and L. A. Chua, "Chaos from phase-locked loops, part II: High dissipation case," *IEEE Trans. Circuits Syst.*, vol. 36, pp. 225–263, 1989.
[10] T. Endo and L. A. Chua, "Bifurcation diagrams and fractal basin boundaries of phase-locked loop circuits," *IEEE Trans. Circuits Syst.*, vol. 37, pp. 534–540, 1990.
[11] F. M. A. Salam, J. E. Marsden, and P. P. Varaya, "Chaos and Arnold diffusion in dynamical systems," *IEEE Trans. Circuits Syst.*, vol. 30, pp. 697–708, 1983.
[12] J. Guckenheimer and P. J. Holmes, *Nonlinear Oscillations, Dynamical Systems, and Bifucation of Vector Fields*, New York-EUA, Springer-Verlag, 1983.
[13] S. Wiggins, *Introduction to Applied Nonlinear Dynamical Systems and Chaos*, New York-EUA, Springer-Verlag, 1990.
[14] K. Ogata, *Modern Control Engineering*, New Jersey, Prentice-Hall, 1997.
[15] L. H. A. Monteiro, D. N. Favaretto Filho, and J. R. C. Piqueira, "Bifurcation analysis for third-order phase-locked loops," *IEEE Signal Processing Lett.*, vol. 11, no. 5, pp. 494–496, 2004.
[16] J. Carr, *Applications of Centre Manifold Theory*, New York-EUA, Springer-Verlag, 1981.

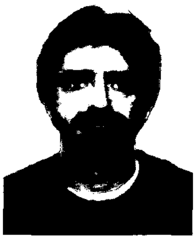

José Roberto Castilho Piqueira was born in Sorocaba, SP, Brazil, in 1952. He received the BsC, MsC, and Ph.D. degrees in electrical engineering in University of São Paulo in 1974, 1983, and 1987, respectively. He is currently a full-professor at Escola Politécnica from University of São Paulo and his research interests include synchronization of electronic and biological oscillations.

Carlos Nehemy Marmo was born in São Paulo, SP, Brazil, in 1974. He received the BsC in civil engineering and the MsC in electrical engineering in University of São Paulo in 2000 and 2003, respectively. He is currently a Ph.D. student at Escola Politécnica from University of São Paulo.

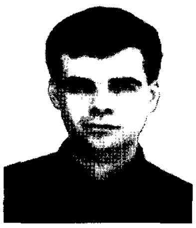

Luiz Henrique Alves Monteiro was born in São Paulo, SP, Brazil, in 1967. He received BsC, MsC, and Ph.D. degrees in physics in Instituto de Física da Universidade de São Paulo in 1987, 1990, and 1995, respectively. He is currently professor/researcher at the Universidade Presbiteriana Mackenzie and University of São Paulo. His present research interests include studies about the behaviors appearing in networks of biological and electronic oscillators.